A family of finite-temperature electronic phase transitions in graphene multilayers

Nam, Young Woo; Ki, Dongkeun; Soler Delgado, David; Morpurgo, Alberto

How to cite

NAM, Young Woo et al. A family of finite-temperature electronic phase transitions in graphene multilayers. In: Science, 2018, vol. 362, n° 6412, p. 324–328. doi: 10.1126/science.aar6855

This publication URL: https://archive-ouverte.unige.ch/unige:151984
Publication DOI: 10.1126/science.aar6855

A Family of Finite-Temperature Electronic Phase Transitions in Graphene Multilayers

One Sentence Summary: Electrons in Bernal multilayers undergo a phase transition whose critical temperature increases with increasing thickness.

Youngwoo Nam, Dong-Keun Ki, David Soler-Delgado, and Alberto F. Morpurgo*

Department of Quantum Matter Physics (DQMP) and Group of Applied Physics (GAP), University of Geneva, 24 Quai Ernest-Ansermet, CH1211 Genéve 4, Switzerland.

* Correspondence to: alberto.morpurgo@unige.ch

Abstract:

Suspended Bernal-stacked graphene multilayers up to an unexpectedly large thickness exhibit a broken-symmetry ground state, whose origin remains to be understood. Here we show that a finite-temperature second order phase transition occurs in multilayers whose critical temperature T_c increases from 12 K in bilayers to 100 K in heptalayers. The data provide strong evidence that the transition is associated to the appearance of a self-consistent valley- and spin-dependent staggered potential changing sign from one layer to the next, appearing at T_c and increasing upon cooling in a way described well by mean-field theory. The remarkably systematic evolution with thickness of several measured quantities imposes constraints for any microscopic theory aiming at analyzing the nature of the electronic correlations. It also provides indications as to the thickness at which the behavior of Bernal-stacked multilayers should cross over to that of bulk graphite.

Main text:

Clean two-dimensional conductors in the presence of a large perpendicular magnetic field are strongly correlated systems. Their ground states are determined by Coulomb repulsion between electrons and are characterized by broken symmetries and non-trivial topological invariants that depend sensitively on electron density (n) and applied field (B) (*1-4*). Accordingly, a series of quantum phase transitions occurs upon varying n and B, which manifest themselves in the very rich phenomenology ubiquitously observed in magneto-transport measurements (*5-13*). These considerations hold true irrespective of the specific 2D conductor considered, because they virtually only rely on the formation of Landau levels that quench the electron kinetic energy, and allow electron-electron (*e-e*) interactions to dominate. In the absence of Landau levels, however, *e-e* interactions play a much less prominent role. Indeed, in these same systems exhibiting quantum Hall effect at finite B, no unambiguous evidence for a $B = 0$ electronic phase transition driven by Coulomb repulsion has been reported despite decades of research.

Different recent experiments indicate that in graphene multilayers the situation is different (*14-19*). Here we focus on ultra-clean, suspended Bernal-stacked multilayers near charge neutrality and show that these systems unambiguously exhibit an *e-e* driven finite-temperature phase transition to a broken symmetry state at a critical temperature T_c that depends on thickness. The transition occurs in all multilayers, but whereas even multilayers become fully insulating for $T \ll T_c$, in odd multilayers a finite conductivity of $\sim e^2/h$ persists down to the lowest temperature reached in the experiments. In the broken-symmetry state, all experimental observations can be accounted for by the appearance of a staggered valley- and spin-dependent potential Δ changing sign from one layer to the next, acting as an order parameter (*18, 19*). The temperature dependence of the order parameter inferred from the data agrees with the one expected for a mean-field second-order phase transition, with Δ decreasing continuously as temperature is increased and vanishing at T_c. Unexpectedly, T_c increases systematically upon increasing the thickness of the multilayer, starting at $T_c = 12$ K for bilayer graphene (2LG) and reaching up to $T_c = 100$ K for heptalayer graphene (7LG), the thickest multilayer in which we have succeeded in observing the phase transition directly. Our experiments therefore demonstrate that charge neutral Bernal-stacked graphene multilayers are a unique family of strongly correlated systems even at $B = 0$.

A gapped insulating state at $B = 0$, first reported in Bernal-stacked bilayers (*14-17*), has been recently observed in all even Bernal-stacked multilayers up to octalayer graphene (8LG) (*18, 19*). In contrast, odd Bernal-stacked multilayers (so far mono and trilayer have been studied) remain conducting at low temperature (*20-23*). These findings defy common expectations, namely that the behavior of graphene multilayers should approach that of graphite as thickness is increased. No direct information about the nature of the insulating state in even multilayers could be obtained so far, because the phenomenon is only observed in suspended graphene devices of the highest quality (*14-23*), which makes it extremely challenging to perform measurements other than transport. Since, upon cooling, the resistance of even multilayers increases without showing abrupt changes at any specific temperature, experiments do not even allow us to tell whether the insulating state results from a quantum phase transition (with a gap present at all temperatures), or if a phase transition occurs at a critical temperature T_c with the gap vanishing for $T > T_c$ (*16, 17, 24-28*). At this stage, the investigation of an experimentally accessible physical quantity that provides more direct information about the low-energy density of states (DOS) is becoming essential.

We have identified such a quantity in the density of electrons present in the conduction band of charge-neutral multilayers, $n_{th}(T)$, whose temperature dependence is indeed determined by the low-energy DOS. At sufficiently low T, $n_{th}(T)$ should show an exponential increase in the presence of gap –since at charge neutrality electrons in the conduction band are thermally activated from the valence band– or stay constant if an overlap between valence and conduction band is present. If the multilayers are zero-band gap semiconductors, $n_{th}(T)$ is expected to increases with increasing T, with a specific dependence determined entirely by the low-energy DOS. In all cases, quantitative information can be obtained by comparing experimental data to the dependence of $n_{th}(T)$ calculated from a chosen theoretical expression for the low-energy DOS, as we illustrate for the case of bilayers. Under the assumption that only the nearest neighbor in-plane (γ_0) and out-of-plane (γ_1) hopping terms are relevant (the so-called minimal tight-binding model), the low-energy quadratic dispersion relation of electrons in bilayer graphene (Figure 1A) leads to an energy-independent DOS (Figure 1B). The resulting density $n_{th}(T)$ of electrons in the conduction band then increases linearly with temperature (Figure 1C). However, if a gap Δ opens (Figure 1D), the DOS is modified

(Figure 1E), and so is the temperature dependence of $n_{th}(T)$. Figure 1F shows $n_{th}(T)$ expected for a gap Δ exhibiting a mean-field temperature dependence and vanishing at T_c (see the inset and (*29*)). A transition becomes visible at $T = T_c$, below which $n_{th}(T)$ is pronouncedly suppressed as compared to the non-interacting case.

What makes these considerations useful is that the extremely small charge inhomogeneity due to disorder present in suspended graphene multilayers enables the density $n_{th}(T)$ of thermally excited electrons to be determined experimentally over a broad range of temperatures. $n_{th}(T)$ can be extracted from the density dependence of the conductance $G(n)$ near charge neutrality. To understand physically why and how, it is useful to look at the double logarithmic plot of $G(n)$ (inset of Fig. 1G). We see that there is a range of n over which $log(G)$ is constant, and that $log(G)$ starts increasing significantly only when n becomes larger than a threshold (that we denote $n^*(T)$*;* $n^*(T)$ increases at higher T). The physical reason is clear: the square conductance remains virtually unchanged as long as the density n of electrons accumulated by the gate voltage is much smaller than the density of electrons already present $n_{th}(T)$ due to thermal activation from the valence band. Finding that the square conductance increases significantly only when n exceeds $n^*(T)$ therefore implies that $n_{th}(T) \sim n^*(T)$, as discussed in several occasions in the past for mono- and bi-layer graphene (*21, 30-32*). In practice, the exact value of $n^*(T)$ depends on the criterion used for its definition: here we define $n^*(T)$ as the value of n for which the conductivity $\sigma(n,T) = 1.67\sigma(n=0,T)$, a relation that we can validate for bilayers and that is approximately correct for thicker multilayers (*29*). We emphasize, however, that none of our key conclusions depends on the precise criterion used (*29*).

The temperature dependence of $n^*(T)$ extracted from measurements on four different bilayer devices is shown in Figure 1G. For all devices, a critical temperature $T_c \cong 12$ K is found, below which $n^*(T)$ is suppressed as compared to the gapless case. The red continuous curve, which represent $n_{th}(T)$ expected for a gap having a mean-field temperature dependence and $\Delta_0 = \Delta(T = 0) \cong 1.9$ meV, reproduces the data very satisfactorily. The presence of a clear transition below which a finite Δ appears, the value of T_c, and the shape of $n^*(T)$ are very robust against all aspects

of the data analysis. They can be extracted directly from the data without any assumption about the DOS, and do not depend on the criterion used to extract $n^*(T)$ (only the quantitative determination of Δ does require the DOS to be specified, see (*29*)). Remarkably, the same value for the critical temperature is found in all the different devices measured, despite the fact that the absolute value of the low-temperature resistance –and how pronounced the insulating state is at the lowest temperature of our measurements– exhibit much larger sample-to-sample fluctuations (because of these fluctuations, even just the occurrence of an insulating state driven by *e-e* interaction has been questioned in some past experimental work (*14-17, 30, 33*)). The reason for this excellent reproducibility is that our measurements effectively probe the DOS averaged over the entire device area, whereas in the insulating state the absolute value of the resistance is strongly affected by any percolating conducting path (e.g. at edges (*34, 35*)) that occupies a negligible fraction of the total area, giving a negligible contribution to the DOS. The highly reproducible behavior of $n^*(T)$ allows us to establish unambiguously the occurrence of an insulating, gapped state near charge neutrality, which is entered through a second-order phase transition at T_c = 12 K.

The same strategy outlined for bilayers can be applied to thicker even multilayers, in which multiple conduction and valence bands are present (*29, 36-39*). Recent work (specifically, the quantization of the Hall effect at low magnetic field and magneto-Raman experiments) has provided evidence that in suspended devices at low energy these bands are well described by including only nearest neighbor in plane (γ_0) and out of plane (γ_1) hopping terms (*18, 19, 40, 41*). According to this description, all conduction and valence bands in even multilayers are quadratic at low energy (with different effective masses), so that the DOS in the non-interacting case is again energy-independent (see (*29*)). The same argument used for bilayers implies that $n_{th}(T)$ increases linearly with temperature in the absence of interactions, and that the opening of a gap causes a suppression for $T < T_c$. Figure 2A and 2C illustrate the results of experiments performed on tetralayer (4LG) and hexalayer (6LG) graphene devices: indeed $n^*(T)$ depends linearly on temperature at sufficiently high temperature, but below a critical temperature T_c (= 38 K for 4LG and 90 K for 6LG) $n^*(T)$ is suppressed, just as for bilayers (Figure 2F and 2G). Also for 4LG and 6LG, the data are excellently reproduced by assuming that a gap Δ with a mean-field temperature dependence opens simultaneously at T_c on all quadratic bands (red line; $\Delta_0 \cong 5.2$ meV for 4LG

and $\Delta_0 \cong 13$ meV for 6LG). Again, the temperature dependence of the resistance at charge neutrality (Figure 2B and 2D) demonstrates the insulating nature of thicker even multilayers, but provides no specific feature allowing the identification of a critical temperature.

The analysis of the measured temperature dependence of $n^*(T)$ and the comparison with the calculated expression for $n_{th}(T)$ can be performed – and interpreted in the same way– also for odd Bernal multilayers. Within the minimal tight-binding model mentioned above, odd multilayers contain multiple conduction and valence bands, all having a quadratic dispersion, except for one that is a linear Dirac band (*29, 36-39*). The DOS associated to the linear band vanishes at charge neutrality, and contributes at most a few percent of the total DOS in the temperature and density range relevant for our work (*29*). It is therefore negligible in practice, so that the same considerations made for even multilayers hold true for odd ones. In Figure 3, data measured on odd Bernal-stacked multilayers show that this is indeed the case for both trilayer (3LG, Figure 3A) and heptalayer graphene (7LG, Figure 3C): $n^*(T)$ increases linearly with temperature at high temperature, exhibiting a pronounced suppression for $T < T_c$ (with $T_c = 33$ K for 3LG and 100 K for 7LG), in complete analogy to the case of even multilayers. Also for odd multilayers, the data agree quantitatively with the behavior expected if a gap Δ opens simultaneously at T_c in all quadratic bands, with a mean-field temperature dependence and $T = 0$ values of $\Delta_0 \cong 5$ meV for 3LG and $\Delta_0 \cong 13$ meV for 7LG. Note that for odd multilayers the low-temperature conductivity remains finite, $\sigma \sim e^2/h$, indicating that the linear band does not gap out (Figure 3B and 3D).

In summary, our findings show that a phase transition occurs in all the Bernal-stacked multilayer investigated, irrespective of whether they are even or odd, with only the even ones becoming insulating at low temperature. Data for multilayers of all thicknesses are shown in Figure 4A– each with the corresponding fit to the calculated temperature dependence of the density of thermally activated electrons $n_{th}(T)$. Remarkably, if $n^*(T)/n^*(T_c)$ is plotted versus T/T_c (i.e., if normalized variables are used), all data collapse on top of each other (see the inset of Figure 4A). T_c increases linearly with increasing thickness (see Figure 4B) and so does the gap Δ_0, that is proportional to

T_c (Figure 4C): the best linear fit –continuous line– is close to the expected mean-field value, $\Delta_0/k_BT_c = 1.76$ –dashed line.

The experimental findings consistently provide substantial evidence about the microscopic nature of the broken-symmetry state, namely that the effect of interactions is well described by a (valley- and spin-dependent) mean-field staggered potential changing sign from one layer to the next, acting as an order parameter (*18, 19*). A scenario based on the minimal tight-binding model augmented with a self-consistent staggered potential explains *i)* that at low temperature even multilayers become fully insulating whereas in odd ones a finite conductivity of $\sim e^2/h$ persists (see Figure 2B, 2D and Figure 3B, 3D); *ii)* that from 1LG to 8LG the first quantum Hall plateau appears systematically at filling factor $\nu = 2N$ with $\sigma_{xy} = 2Ne^2/h$, where N is the multilayer thickness (see (*18, 19*)); *iii)* the occurrence of the transition in odd multilayers; *iv)* that the gap in the different quadratic bands has the same magnitude; *v)* the simultaneous opening of the gap in all bands at a same critical temperature (indeed, inasmuch *iv)* and *v)* are concerned, a generic mechanism could gap each band independently from the others, resulting in multiple transitions with different values of T_c and Δ (*42, 43*)). Note, finally, that in the scenario that we propose –with the staggered potential acting as order parameter– the symmetry broken is discrete, which is why the occurrence of finite-temperature phase transitions in Bernal multilayers does not conflict with the Mermin-Wagner theorem (*44*), despite all multilayers being effectively two-dimensional.

We conclude that an interpretation in terms of the minimal tight-binding model augmented by a (valley and spin dependent) staggered potential is very successful and finding a drastically different scenario capable of accounting for all experimental observations seems difficult. However, in the absence of a comprehensive theoretical analysis important questions remain. A key one is the validity of the minimal tight-binding model since –based on the vast existing literature on graphite– it may be expected that more tight-binding parameters should be included. In this regard we note that a recent theoretical analysis of *e-e* interaction at the Hartree-Fock level (*43*) show that adding hopping terms present in graphite –and most notably the parameter γ_2, responsible for the semi-metallic behavior of graphite ($\gamma_2 \sim$ -20 meV usually)– would make the

systematic behavior observed in multilayers impossible to reproduce theoretically: no even-odd effect of the conductivity would be expected and the insulating gap would decrease rapidly with increasing thickness (the same calculations with $\gamma_2 = 0$, instead, would come closer to reproducing the experimental observations, except the linear increase of Δ with thickness; see also (*42*)). Additionally, $\gamma_2 \sim$ -20 meV would also strongly affect the $E = 0$ Landau level and would not be compatible with the observed first quantum Hall plateau, which in *N*-layer is found to occur at filling factor $\nu = 2N$ with $\sigma_{xy} = 2Ne^2/h$. At the simplest level the same holds true for other hopping parameters, e.g., γ_3, responsible for trigonal warping. Why some hopping terms that must be included to describe graphite do not appear in thin multilayers requires an explanation. We believe that a key difference is that our experiments probe charge neutral multilayers (i.e., $n \sim 0$), whereas in graphite approximately $n \sim$ 3-4 10^{11} electrons/cm^2 are present in each individual layer (*45*). Indeed it has been established theoretically and experimentally that, as *n* approaches charge neutrality, large renormalization effects drastically change the hopping parameters in graphene: in monolayers, for instance, the Fermi velocity (and hence γ_0) is predicted to diverge as $n \rightarrow 0$ (*22, 46-48*). Although a thorough analysis of this renormalization process for all hopping parameters is lacking, what is known at this stage implies that there is no compelling reason why the hopping terms used to describe graphite and charge neutral thin multilayers should be the same, i.e., using the minimal tight binding model is not in conflict with earlier work on graphite.

Irrespective of these details, what is most remarkable in the experimental findings is the occurrence of a phase transition with increasingly large T_c in graphene multilayers that, until now, may have been expected to behave as bulk graphite. Why precisely T_c increases with increasing thickness or at which thickness this trend breaks down, and the behavior of bulk graphite recovered, remains to be understood. As we discuss in (*29*), the experimental observations are so systematic to give indications on these points. However, only a thorough microscopic theoretical analysis will allow the properties of this family of electronic systems to be understood in detail, disclosing its full potential to reveal subtle phenomena emerging from the physics of correlated electrons.

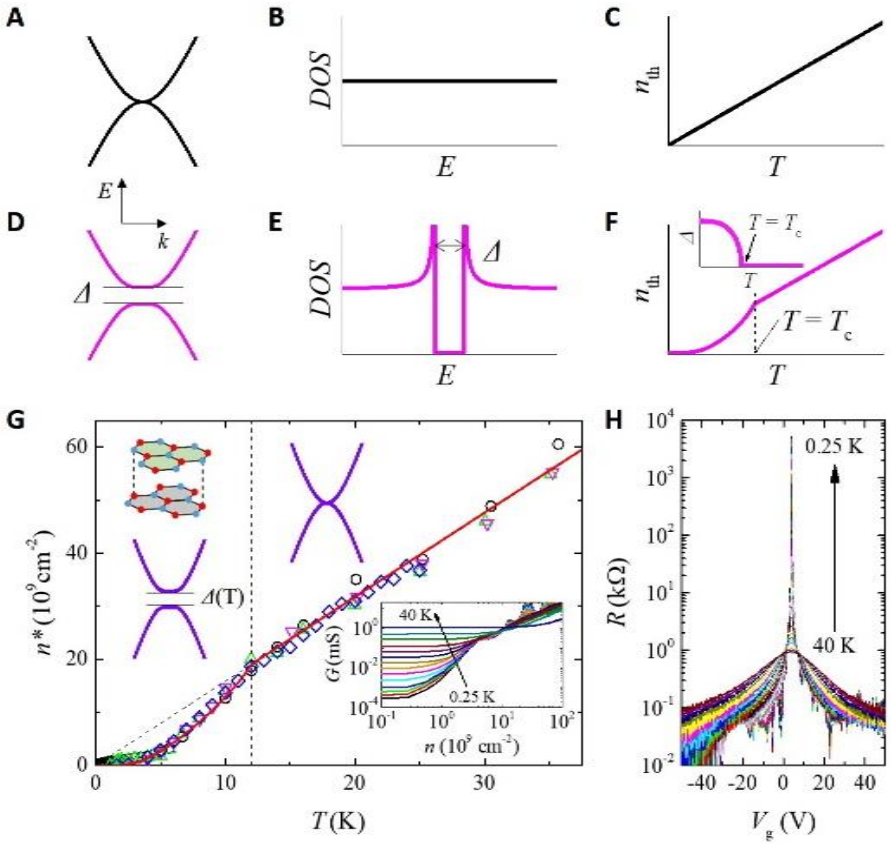

Fig. 1. Electronic phase transition in bilayer graphene (2LG). In the absence of interactions, Bernal-stacked graphene bilayers are zero-gap semiconductors with valence and conduction bands dispersing quadratically at low energy (**A**), resulting in a constant DOS (**B**). As a result, the density of electrons thermally excited from the conduction to the valence band, $n_{th}(T)$, increases linearly with temperature (**C**). The opening of a gap (Δ) due to interactions (**D**) leads to a modified DOS (**E**) and causes a suppression of $n_{th}(T)$ (**F**) (the inset shows $\Delta(T)$ expected from a mean-field description, used to calculate $n_{th}(T)$). The different symbols in (**G**) represent $n^*(T)$ (~ $n_{th}(T)$ as discussed in the main text and (*29*)) measured on four distinct bilayer devices, all showing a transition at T_c = 12 K. Above T_c, the value of the slope of $n^*(T)$ matches the one expected from the known DOS of 2LG (i.e., effective mass). The red line is a fit to the expression for $n_{th}(T)$ calculated with a mean-field temperature dependence of $\Delta(T)$. The bottom inset shows the double logarithmic plot of $G(n)$ measured at different values of T, from which $n^*(T)$ is extracted. The gate-voltage dependence of the resistance of this same device is shown in (**H**) for different temperatures. It exhibits a pronounced insulating behavior around charge neutrality, but no indications of a phase transition.

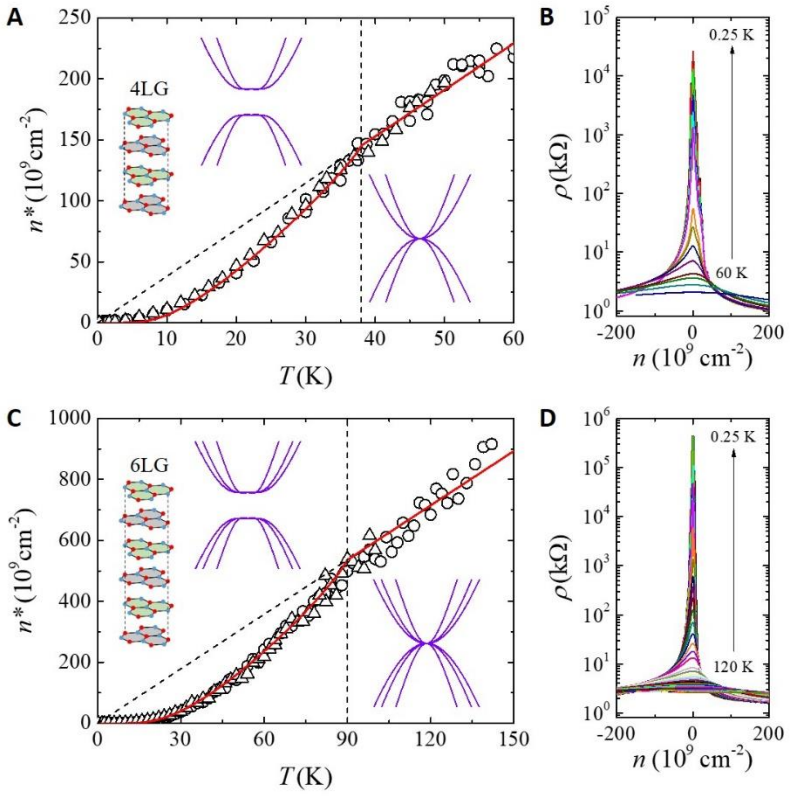

Fig. 2. Electronic phase transition in even Bernal-stacked multilayers. Panel (A)-(B) and (C)-(D) show data measured on tetralayer (4LG) and hexalayer graphene (6LG), respectively. (**A**) and (**C**) show that at sufficiently high temperature the measured $n^*(T)$ depends linearly on T. Below the critical temperature T_c (= 38 K for 4LG and 90 K for 6LG) $n^*(T)$ is suppressed as found in bilayers (see Fig. 1). The red continuous curves in (A) and (C), which correspond to the dependence of $n_{th}(T)$ expected for a gap having a mean-field temperature dependence, reproduce the data very satisfactorily. In (A) and (C), the circles and tringles represent data obtained from different devices, demonstrating the excellent reproducibility of our observations. (**B**), (**D**) Charge carrier density dependence of the resistivity at different temperatures, showing an insulating state around charge neutrality at low temperature. As for bilayers, in the temperature dependence of the resistance no sharp feature is seen that allows the value of T_c to be determined experimentally. Note that the asymmetry visible for positive and negative values of n is due to the formation of a *pn* junction at the contacts, as typically observed in two-terminal suspended graphene devices. In all multilayers for which four-terminal devices (*49*) could be realized the resistivity is nearly perfectly symmetric upon changing the sign of n (see, e.g., Fig. 1(**H**) and 3(**B**)).

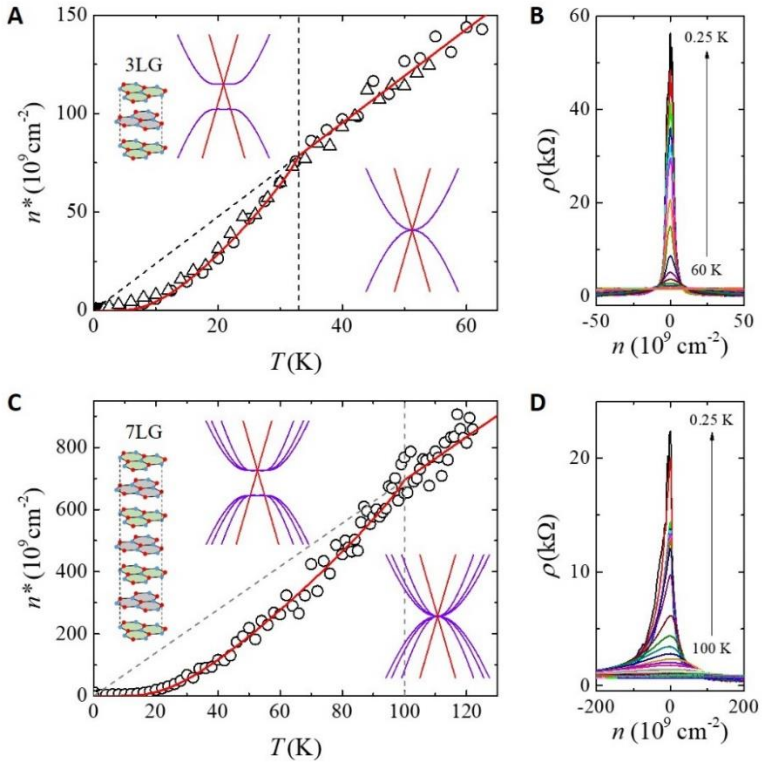

Fig. 3. Electronic phase transition in odd Bernal-stacked multilayers. Panel (**A**)-(**B**) and (**C**)-(**D**) show data measured on trilayer (3LG) and heptalayer graphene (7LG). (**A**) and (**C**) show that the temperature dependence of $n^*(T)$ is linear at sufficiently high T, just as observed for even layers, because the DOS associated to the Dirac linear band present in odd layers is negligible in the energy range probed by the experiments. For temperatures below T_c (=33 K for 3LG and 100 K for 7LG) $n^*(T)$ is suppressed, in a way identical to that observed in even layers, demonstrating that all the quadratic bands gap out for $T < T_c$. Also for odd layers, $n^*(T)$ is well reproduced by the temperature dependent density of electrons thermally excited from the valence to the conduction band – the red continuous curves– calculated assuming a mean-field gap. In (**A**), the circles and the tringles represent data obtained from two different devices, demonstrating once more excellent reproducibility. (**B**), (**D**) Charge carrier density dependence of the resistivity at different temperatures, showing a finite low-temperature conductivity of ~ e^2/h around charge neutrality, due to the presence of the linear band that remains un-gapped (the 3LG data in (**B**), measured on a four-terminal device, are nearly perfectly symmetric in n; for the 7LG device in (**D**) the asymmetry is due to the two-terminal device configuration).

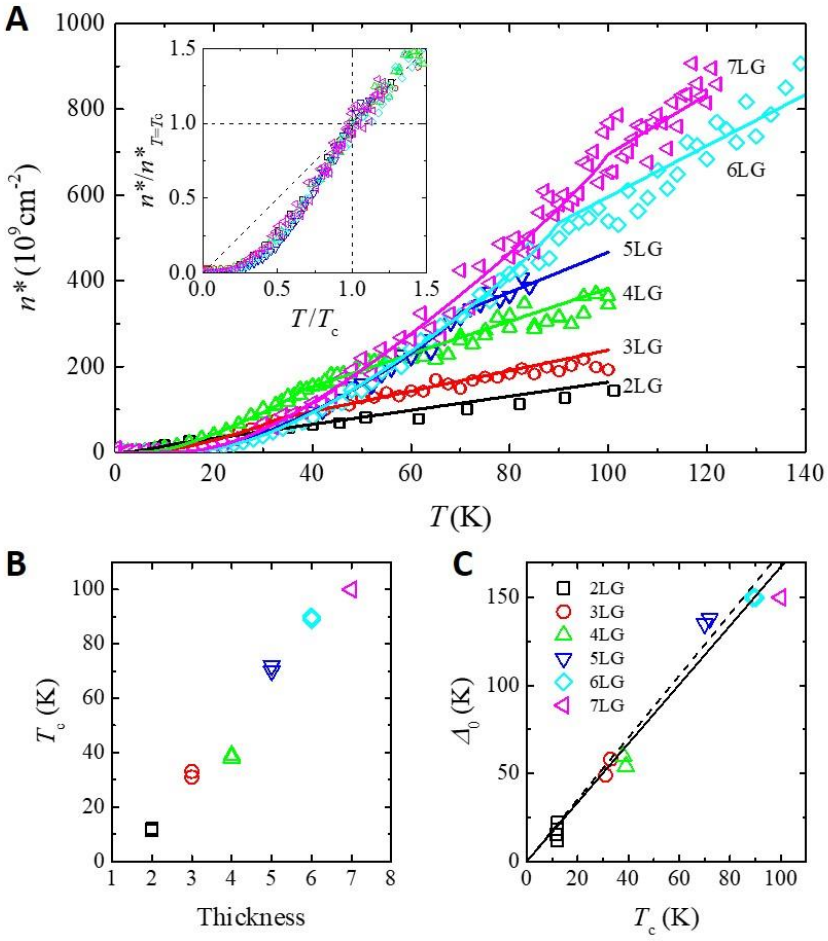

Fig. 4. Evolution with thickness of the phase transition to the broken-symmetry state. (**A**) n^* versus temperature for Bernal-stacked multilayers of all thicknesses, from bi to heptalayer graphene. The continuous lines of the corresponding color are obtained by fitting the theoretical expression for the temperature dependence of the density of electron thermally excited from the valence to the conduction band, $n_{th}(T)$, calculated using a mean-field temperature dependence for the gap. The inset shows that when looked at in terms of normalized quantities –i.e., $n^*(T)/n^*(T_c)$ is plotted versus T/T_c– all curves collapse on top of each other. For every thickness, only one critical temperature is observed and only one value of the gap is needed to reproduce the data, indicating that a gap opens simultaneously in all quadratic bands. (**B**) T_c increases linearly with increasing thickness and the gap Δ_0 is proportional to T_c (**C**). The best linear fit –continuous line– is close to the relation expected from mean-field theory, $\Delta_0/k_BT_c = 1.76$ –dashed line.

Acknowledgments:

We gratefully acknowledge A. Ferreira for continued technical support of the experiments and T. Giamarchi for useful discussions. Financial support from the Swiss National Science Foundation, the NCCR QSIT, and the EU Graphene Flagship Project are also gratefully acknowledged.

Supplementary Materials:

Materials and Methods

Figures S1-S11

References (##-##):

References and Notes:

1. D. Yoshioka, *The Quantum Hall Effect*. (Springer, Berlin, 2002).
2. J. K. Jain, *Composite Fermions*. (Cambridge University Press, Cambridge 2007).
3. Z. F. Ezawa, *Quantum Hall Effects: Field Theoretical Approach and Related Topics*. (World Scientific, Singapore, 2008).
4. E. Fradkin, *Field Theories of Condensed Matter Physics*. (Cambridge University Press, Cambridge 2013).
5. D. C. Tsui, H. L. Stormer, A. C. Gossard, Two-Dimensional Magnetotransport in the Extreme Quantum Limit. *Phys. Rev. Lett.* **48**, 1559-1562 (1982).
6. R. Willett, J. P. Eisenstein, H. L. Störmer, D. C. Tsui, A. C. Gossard, J. H. English, Observation of an even-denominator quantum number in the fractional quantum Hall effect. *Phys. Rev. Lett.* **59**, 1776-1779 (1987).
7. J. P. Eisenstein, A. H. MacDonald, Bose–Einstein condensation of excitons in bilayer electron systems. *Nature* **432**, 691–694 (2004).
8. P. Maher, C. R. Dean, A. F. Young, T. Taniguchi, K. Watanabe, K. L. Shepard, J. Hone, P. Kim, Evidence for a spin phase transition at charge neutrality in bilayer graphene. *Nat. Phys.* **9**, 154 (2013).
9. A. F. Young, J. D. Sanchez-Yamagishi, B. Hunt, S. H. Choi, K. Watanabe, T. Taniguchi, R. C. Ashoori, P. Jarillo-Herrero, Tunable symmetry breaking and helical edge transport in a graphene quantum spin Hall state. *Nature* **505**, 528–532 (2013).
10. D.-K. Ki, V. I. Fal'ko, D. A. Abanin, A. F. Morpurgo, Observation of Even Denominator Fractional Quantum Hall Effect in Suspended Bilayer Graphene. *Nano Lett.* **14**, 2135-2139 (2014).
11. J. Falson, D. Maryenko, B. Friess, D. Zhang, Y. Kozuka, A. Tsukazaki, J. H. Smet, M. Kawasaki, Even-denominator fractional quantum Hall physics in ZnO. *Nat. Phys.* **11**, 347–351 (2015).
12. A. A. Zibrov, C. Kometter, H. Zhou, E. M. Spanton, T. Taniguchi, K. Watanabe, M. P. Zaletel, A. F. Young, Tunable interacting composite fermion phases in a half-filled bilayer-graphene Landau level. *Nature* **549**, 360–364 (2017).
13. J. I. A. Li, C. Tan, S. Chen, Y. Zeng, T. Taniguchi, K. Watanabe, J. Hone, C. R. Dean, Even-denominator fractional quantum Hall states in bilayer graphene. *Science* **358**, 648-652 (2017).
14. R. T. Weitz, M. T. Allen, B. E. Feldman, J. Martin, A. Yacoby, Broken-Symmetry States in Doubly Gated Suspended Bilayer Graphene. *Science* **330**, 812-816 (2010).
15. F. Freitag, J. Trbovic, M. Weiss, C. Schönenberger, Spontaneously Gapped Ground State in Suspended Bilayer Graphene. *Phys. Rev. Lett.* **108**, 076602 (2012).
16. J. Velasco Jr, L. Jing, W. Bao, Y. Lee, P. Kratz, V. Aji, M. Bockrath, C. N. Lau, C. Varma, R. Stillwell, D. Smirnov, F. Zhang, J. Jung, A. H. MacDonald, Transport spectroscopy of symmetry-broken insulating states in bilayer graphene. *Nat. Nanotechnol.* **7**, 156–160 (2012).
17. W. Bao, J. Velasco, F. Zhang, L. Jing, B. Standley, D. Smirnov, M. Bockrath, A. H. MacDonald, C. N. Lau, Evidence for a spontaneous gapped state in ultraclean bilayer graphene. *Proc. Natl. Acad. Sci. U.S.A.* **109**, 10802-10805 (2012).

18. A. L. Grushina, D.-K. Ki, M. Koshino, A. A. L. Nicolet, C. Faugeras, E. McCann, M. Potemski, A. F. Morpurgo, Insulating state in tetralayers reveals an even–odd interaction effect in multilayer graphene. *Nat. Commun.* **6**, 6419 (2015).
19. Y. Nam, D.-K. Ki, M. Koshino, E. McCann, A. F. Morpurgo, Interaction-induced insulating state in thick multilayer graphene. *2D Mater.* **3**, 045014 (2016).
20. K. I. Bolotin, K. J. Sikes, Z. Jiang, M. Klima, G. Fudenberg, J. Hone, P. Kim, H. L. Stormer, Ultrahigh electron mobility in suspended graphene. *Solid State Commun.* **146**, 351-355 (2008).
21. X. Du, I. Skachko, A. Barker, E. Y. Andrei, Approaching ballistic transport in suspended graphene. *Nat. Nanotechnol.* **3**, 491–495 (2008).
22. D. C. Elias, R. V. Gorbachev, A. S. Mayorov, S. V. Morozov, A. A. Zhukov, P. Blake, L. A. Ponomarenko, I. V. Grigorieva, K. S. Novoselov, F. Guinea, A. K. Geim, Dirac cones reshaped by interaction effects in suspended graphene. *Nat. Phys.* **7**, 701-704 (2011).
23. W. Bao, L. Jing, J. Velasco, Y. Lee, G. Liu, D. Tran, B. Standley, M. Aykol, S. B. Cronin, D. Smirnov, M. Koshino, E. McCann, M. Bockrath, C. N. Lau, Stacking-dependent band gap and quantum transport in trilayer graphene. *Nat. Phys.* **7**, 948-952 (2011).
24. R. Nandkishore, L. Levitov, Dynamical Screening and Excitonic Instability in Bilayer Graphene. *Phys. Rev. Lett.* **104**, 156803 (2010).
25. Y. Lemonik, I. L. Aleiner, C. Toke, V. I. Fal'ko, Spontaneous symmetry breaking and Lifshitz transition in bilayer graphene. *Phys. Rev. B* **82**, 201408 (2010).
26. F. Zhang, H. Min, M. Polini, A. H. MacDonald, Spontaneous inversion symmetry breaking in graphene bilayers. *Phys. Rev. B* **81**, 041402 (2010).
27. F. Zhang, J. Jung, G. A. Fiete, Q. Niu, A. H. MacDonald, Spontaneous Quantum Hall States in Chirally Stacked Few-Layer Graphene Systems. *Phys. Rev. Lett.* **106**, 156801 (2011).
28. F. Zhang, A. H. MacDonald, Distinguishing Spontaneous Quantum Hall States in Bilayer Graphene. *Phys. Rev. Lett.* **108**, 186804 (2012).
29. See supplementary materials on Science Online.
30. A. S. Mayorov, D. C. Elias, M. Mucha-Kruczynski, R. V. Gorbachev, T. Tudorovskiy, A. Zhukov, S. V. Morozov, M. I. Katsnelson, V. I. Fal'ko, A. K. Geim, K. S. Novoselov, Interaction-Driven Spectrum Reconstruction in Bilayer Graphene. *Science* **333**, 860-863 (2011).
31. A. S. Mayorov, D. C. Elias, I. S. Mukhin, S. V. Morozov, L. A. Ponomarenko, K. S. Novoselov, A. K. Geim, R. V. Gorbachev, How Close Can One Approach the Dirac Point in Graphene Experimentally? *Nano Lett.* **12**, 4629-4634 (2012).
32. J. Crossno, J. K. Shi, K. Wang, X. Liu, A. Harzheim, A. Lucas, S. Sachdev, P. Kim, T. Taniguchi, K. Watanabe, T. A. Ohki, K. C. Fong, Observation of the Dirac fluid and the breakdown of the Wiedemann-Franz law in graphene. *Science* **351**, 1058-1061 (2016).
33. P. San-Jose, R. V. Gorbachev, A. K. Geim, K. S. Novoselov, F. Guinea, Stacking Boundaries and Transport in Bilayer Graphene. *Nano Lett.* **14**, 2052-2057 (2014).
34. J. Li, I. Martin, M. Buttiker, A. F. Morpurgo, Topological origin of subgap conductance in insulating bilayer graphene. *Nat. Phys.* **7**, 38-42 (2011).
35. M. J. Zhu, A. V. Kretinin, M. D. Thompson, D. A. Bandurin, S. Hu, G. L. Yu, J. Birkbeck, A. Mishchenko, I. J. Vera-Marun, K. Watanabe, T. Taniguchi, M. Polini, J. R. Prance, K. S. Novoselov, A. K. Geim, M. Ben Shalom, Edge currents shunt the insulating bulk in gapped graphene. *Nat. Commun.* **8**, 14552 (2017).

36. F. Guinea, A. H. Castro Neto, N. M. R. Peres, Electronic states and Landau levels in graphene stacks. *Phys. Rev. B* **73**, 245426 (2006).
37. B. Partoens, F. M. Peeters, Normal and Dirac fermions in graphene multilayers: Tight-binding description of the electronic structure. *Phys. Rev. B* **75**, 193402 (2007).
38. M. Koshino, T. Ando, Orbital diamagnetism in multilayer graphenes: Systematic study with the effective mass approximation. *Phys. Rev. B* **76**, 085425 (2007).
39. M. Koshino, E. McCann, Parity and valley degeneracy in multilayer graphene. *Phys. Rev. B* **81**, 115315 (2010).
40. S. Berciaud, M. Potemski, C. Faugeras, Probing Electronic Excitations in Mono- to Pentalayer Graphene by Micro Magneto-Raman Spectroscopy. *Nano Lett.* **14**, 4548-4553 (2014).
41. Y. Henni, H. P. Ojeda Collado, K. Nogajewski, M. R. Molas, G. Usaj, C. A. Balseiro, M. Orlita, M. Potemski, C. Faugeras, Rhombohedral Multilayer Graphene: A Magneto-Raman Scattering Study. *Nano Lett.* **16**, 3710-3716 (2016).
42. C. Yoon, Y. Jang, J. Jung, H. Min, Broken sublattice symmetry states in Bernal stacked multilayer graphene. *2D Mater.* **4**, 021025 (2017).
43. M. Koshino, K. Sugisawa, E. McCann, Interaction-induced insulating states in multilayer graphenes. *Phys. Rev. B* **95**, 235311 (2017).
44. N. D. Mermin, H. Wagner, Absence of Ferromagnetism or Antiferromagnetism in One- or Two-Dimensional Isotropic Heisenberg Models. *Phys. Rev. Lett.* **17**, 1133-1136 (1966).
45. N. B. Brandt, S. M. Chudinov, Y. G. Ponomarev, *Semimetals 1: Graphite and its Compounds* (Elsevier, Amsterdam, 1988).
46. J. González, F. Guinea, M. A. H. Vozmediano, Non-Fermi liquid behavior of electrons in the half-filled honeycomb lattice (A renormalization group approach). *Nucl. Phys. B* **424**, 595-618 (1994).
47. S. Das Sarma, E. H. Hwang, W.-K. Tse, Many-body interaction effects in doped and undoped graphene: Fermi liquid versus non-Fermi liquid. *Phys. Rev. B* **75**, 121406 (2007).
48. M. Polini, R. Asgari, Y. Barlas, T. Pereg-Barnea, A. H. MacDonald, Graphene: A pseudochiral Fermi liquid. *Solid State Commun.* **143**, 58-62 (2007).
49. D.-K. Ki, A. F. Morpurgo, High-Quality Multiterminal Suspended Graphene Devices. *Nano Lett.* **13**, 5165-5170 (2013).